Heliyon 9 (2023) e20927

Contents lists available at ScienceDirect

Heliyon

journal homepage: www.cell.com/heliyon

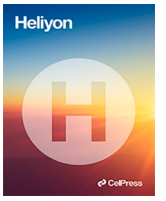

Exergetic analysis of direct contact membrane distillation (DCMD) using PVDF hollow fiber membranes for the desalination brine treatment

Abdul Hanan Muhammad Zaheer [a,b], Lassaad Gzara [a,*], Ahmed Iqbal [a,b], Fransesca Macedonio [c], Mohammed Albeirutty [a,b], Enrico Drioli [c]

[a] Center of Excellence in Desalination Technology, King Abdulaziz University, P.O. Box: 80200, Jeddah 21589, Saudi Arabia
[b] Department of Mechanical Engineering, Faculty of Engineering, King Abdulaziz University, P.O. Box: 80204, Jeddah 21589, Saudi Arabia
[c] National Research Council – Institute on Membrane Technology (CNR-ITM), Via Pietro Bucci cubo 17C, 87036 Rende, CS, Italy

ARTICLE INFO

Keywords:
DCMD
Brine treatment
Exergy
exergetic efficiency
exergy change
Desalination

ABSTRACT

The brines from desalination plants need to be disposed of due to their strong impact on the environment. Membrane operations, like direct contact membrane distillation (DCMD), provide a possible solution to reduce the amount of brine while producing further desalinated water. In this study, an exergy analysis of a laboratory membrane distillation unit working with brines from reverse osmosis (RO) is analyzed. Exergy analysis enables us to assess the energy lost in entropy generation; therefore, it commits us to identify the less efficient configuration of the DCMD module. Unlike other exergy analyses for distillation, in this study, only module inputs and outputs were incorporated. The exergy is calculated at different infeed temperatures, for both in-out and out-in feed configurations of hollow fiber membrane modules. Also, exergy difference, flux, and exergetic efficiency for both configurations are calculated. At high feed temperatures, there is an increase in both flux and exergy change, which increases water recovery and feed side exergetic efficiency. The highest flux that is obtained in the out-in configuration is 13.3 kg/h.m^2 while it is only 6.23 kg/h.m^2 for the in-out system of the module. Also, these exergy changes and feed efficiencies are higher in the out-in module configuration than in the in-out module configuration. Conversely, the exergetic efficiency of the permeate is higher at lower feed temperatures, due to the lower accumulation of concentration polarization along the membrane wall.

1. Introduction

According to the United Nations (UN), global water demand is estimated to increase by 30 % by 2050. Even today, almost 2 billion people experience extreme water shortages throughout the year [1]. Multi-stage flash (MSF), multi-effect distillation (MED), and reverse osmosis (RO) are the most well-known seawater desalination methods. However, in these mentioned processes still about 50% of the concentrated water is discharged into the main streams. With the advent of people's awareness of environmental protection, the ecological environment pollution and hazards faced by offshore and coastal zones by the discharge of concentrated water, are being paid progressively more attention. Therefore, the concentrated drainage to seawater should be controlled [2].

* Corresponding author
E-mail addresses: abdulhanan2112@gmail.com (A.H.M. Zaheer), lgzara@kau.edu.sa (L. Gzara), Francesca.macedonio@unical.it (F. Macedonio).

https://doi.org/10.1016/j.heliyon.2023.e20927
Received 31 May 2023; Received in revised form 9 September 2023; Accepted 11 October 2023
Available online 13 October 2023

The Membrane Distillation (MD) process is a thermally driven process in which the water vapor moves through a porous hydrophobic membrane that serves as a feed-to-permeate partition. In MD, the feed side is always in contact with an aqueous solution, while the permeate side is brought into contact with one of the four phases that give rise to four different types of MD processes: (1) the liquids are in direct contact with both sides of the membrane in direct contact membrane distillation (DCMD); (2) In Sweeping Gas Membrane Distillation (SGMD) incorporates a gas for pure water extraction. (3) Vacuum Membrane Distillation (VMD) uses a vacuum to draw the permeate. (4) Air Gap Membrane Distillation is carried out with a stagnant air gap with a cold plate [2]. DCMD provides numerous benefits in comparison to other distillation procedures. This method's ability to function at lower temperatures results in a decrease in energy consumption and allows for the utilization of waste heat. Additionally, the uncomplicated nature of the process facilitates its operation and maintenance. DCMD membranes offer elevated selectivity and purity, rejecting impurities and liquid to generate premium distillate. The direct contact nature of the process results in reduced scaling and fouling. Moreover, DCMD is adaptable and can process a variety of feed solutions. Its integration with other processes, including reverse osmosis, further enhances its efficiency [3].

Research has concentrated on creating and improving membranes in DCMD. The goal is to improve the process's performance and efficiency by enhancing membrane qualities such as hydrophobicity, porosity, and thermal stability. For their applicability in DCMD, many membrane materials, including polymeric, composite, and nanocomposite membranes, have been studied [4]. Studies have sought to enhance the water flux and reduce energy usage by optimizing the operational DCMD parameters [5]. Researchers have investigated how the performance of DCMD is affected by temperature, feed flow rate, concentration polarization, membrane thickness, and module design. The objective is to maintain process stability while achieving high rates of salt rejection and water recovery [6]. Anari et al., 2019 [7] discussed the difficulties of treating hydraulic fracturing flow back and generated water using direct contact membrane distillation because of fouling by dissolved organic species. According to the study, the performance of membranes can be enhanced by adjusting the characteristics of the monomer units in the polymer chains.

In DCMD, the heated feed, in contact with one side of the membrane, undergoes a phase change, after which it travels through the porous hydrophobic membrane and condenses to produce pure water upon reaching the cold permeate side. Membrane distillation uses heat to evaporate the feed, while low-pressure pumps use electricity. The sources of heat in MD are solar [8], waste heat [9], and district heat [10]. The enormous amount of heat passed via the membrane, which is mostly latent heat but also includes some conductive heat transfer, is largely responsible for the high energy consumption [11]. To increase DCMD's overall effectiveness, researchers have looked into integrating it with other membrane-based processes or energy recovery systems [5]. To reduce energy consumption and improve the economics of the process, hybrid systems have been explored, such as combining DCMD with solar energy or reverse osmosis. DCMD has also been investigated for several applications, such as desalination, wastewater treatment, brine solution concentration, and the recovery of valuable chemicals from industrial effluents [12]. PVDF membranes provide significant benefits in the realm of Direct Contact Membrane Distillation (DCMD). Their intrinsic hydrophobicity impedes the transmission of liquid water, thereby diminishing fouling and augmenting durability. Additionally, PVDF membranes demonstrate impressive thermal stability, thus facilitating elevated operating temperatures that enhance efficacy. They also evince chemical resistance, which enables the treatment of a wide range of feed solutions. The membranes' mechanical robustness ensures stability in the face of pressure differentials. Finally, the ready availability and widespread commercial use of PVDF membranes greatly simplify scalability and implementation [13].

The term exergy in the membrane separation process was first discussed by Molinari et al. [14] in 1995. According to him, the total energy of any system is divided into two parts: anergy and exergy. The part of energy that is called exergy, is converted from one form into another, by reversible transformation. On the othe hand, anergy is that force that is released as a result to overcome degradation. Consequently, exergy refers to the maximum amount of work that can be extracted from any operating system relative to its equilibrium states. He also proposed an equation for calculating the exergy of any system that is discussed in the materials and methods section.

Techno-economic assessments of DCMD have been done to determine its viability and cost-effectiveness for widespread implementation. Research like this compares DCMD to other desalination or water treatment methods in terms of upfront and ongoing expenses, energy usage, and overall performance. The goal is to shed light on whether or not DCMD can be implemented economically and where it might be used. In 2002 Cerci [15] did an exergy analysis of a desalination plant that is working on reverse osmosis located in California, he presented an alternative design to improve the facility's performance based on actual plant operation data. He discovered that the membrane modules (which divide saline water into permeate and brine) lose the most energy (about 74.04%). He evaluated the plant's second law efficiency to be 4.3%. By reducing the pumping power of incoming saline water, the alternative design based on exergy analysis had a second law efficiency of 4.9%, saving 19.8 kW of electricity. Later in 2010, Macedonio and Drioli [16] carried out and compared the exergy analysis of various integrated desalination processes. They calculate the exergy for distinct saline water streams and the distribution of exergy at major system components. Pressure drops in membrane modules, valves, and brine lines are shown to be the principal cause of exergy losses in the plant. To improve the facility's performance and cost, they proposed replacing the valves on the brine streams with energy recovery systems and having the availability of thermal energy in the plant, reducing energy consumption from 18.3 to 2.05 KW/m3.

Recently, Macedonio et al. [12], suggested a series of integrated systems for desalination plants and applied exergy analysis to find energy losses due to entropy production. They put special consideration to the addition of MD and Membrane Crystallization (MCr) for the improvement of water recovery rates and recovery of salts from produced brines. They find a high exergy efficiency of 72 % along with a high water recovery factor of 79 % and brine concentration of 47.6 g/L. A laboratory and pilot-scale exergetic research of air-gap membrane distillation is presented by Woldemariam et al., [6]. AGMD calculated exergy efficiency and exergy destruction using two distinct flat plates and a variety of feed and coolants. The results demonstrate that the MD module is the source of the

system's highest fraction of exergy destruction.

Fakron [17] has done a comparative study on energy and exergy analysis along with modeling temperature distribution in feed channels for VMD and DCMD. In comparison to DCMD, the results showed that VMD has lower energy losses across membrane modules. While the exergy analysis shows that DCMD requires less work input as compared to VMD, in the second part of the research, it can be seen that the temperature polarization phenomena in VMD are less severe than in DCMD. Jihyeok et al. [18], used Computational Fluid Dynamics (CFD) to perform exergetic analysis for direct contact membrane distillation (DCMD). He studied the exergy destruction and temperature polarization at various operating conditions using the CFD model. The results suggested that under higher flux conditions and temperature of feeds, exergy destruction is found to be more significant.

Theoretical investigations on the performance and energy efficiency of the MD process are commonly conducted. Several experimental investigations have been conducted to evaluate the performance of MD systems. As MD is increasingly being used in practical applications, significant developments have been in designing and configuring energy-efficient modules. Exergy, like energy, is lost and can only be saved if all processes in a system and its surroundings are reversible. Exergy destruction is a term that refers to the quantification of irreversibility in any thermodynamic system. As a result, each system's exergetic efficiency is a measure of how close it is to ideality and reversibility. Exergy is related to the heat transfer occurring at any point in a process, such as in membrane distillation (MD). The temperature at which the process takes place, in comparison to the ambient temperature (known as the reference and equilibrium state), is the primary determinant of exergy.

Unlike Macedonio and Drioli's work [16] and that of Macedonio et al. [12], which considers the entire desalination process, including pumps, heaters, and other components, this investigation focuses solely on the membrane distillation process inside the MD module. On the other hand, the potential of hollow fiber membrane-based modules has not been fully investigated yet. This study aims to evaluate the performance of a hollow fiber module in two possible configurations - in-out and out-in - in an MD system. This study confidently evaluates the exergy efficiency of the process by analyzing experimental data obtained from DCMD runs using actual brine from a seawater reverse osmosis plant. The exergy analysis is evaluated as a function of the operating time when the feed solution's total dissolved salts were concentrated. The thermodynamic model used in this study evaluates the exergy efficiency based on the geometry and materials of the module and the membranes.

2. Methodology

2.1. Material

The membranes used in the current work are PVDF hollow fiber membranes manufactured by Econity Co., LTD. (South Korea). The PVDF hollow fiber membrane and module specifications are listed in Table 1. The module has a diameter of 12.5 mm (0.5 inches), UPVC Class 5 type. The number of PVDF membranes used in each module is ten, having an effective length of 20 cm, coupled with tees, installed, and glowed by UPVC glue at both ends of the pipe as shown in Fig. 1. Epoxy is used to isolate both ends of the hollow fiber.

2.2. DCMD performance investigation

The experimental setup for lab-scale DCMD (Fig. 2) was designed and assembled in Italy by DeltaE Srl. The brine solution used in the experiment is brought from the local RO plant. The physical and chemical characterization of the brine solution is depicted in Table 2. The experiments done on DCMD is countercurrent setup with different experimental parameters, such as feed temperature and operating time, which have been studied with different feed configurations i.e., in-out and out-in, to evaluate the performance in terms of flux and exergy evaluation of PVDF membrane in brine treatment. In in-out module configuration the high temperature feed travels in the hollow fiber membranes, while the cold permeate surrounds it in the module. On the other hand, in the out-in module

Table 1
Specification of PVDF hollow fiber membrane used in the experiment.

Specification Parameters	Value
Mean pore size (μm)	0.1
Contact Angle (degrees)	89.4
Porosity (%)	51.9
Liquid Entry Pressure LEP (bar)	2.35
Tensile strength of Membrane (MPa)	14.2
Nominal diameter of fiber (inner) (mm)	0.75
Nominal diameter of fiber (outer) (mm)	1.2
Diameter of Module (mm)	12.5
Module length (m)	0.20
Module membrane area (in-out) (m^2)	0.004712
Module membrane area (out-in) (m^2)	0.007536
Number of fibers	10

Temperature, pressure, and salt concentration are the three important factors for calculating the exergy at any point in the DCMD setup. These parameters are closely followed at the in-feeds and out-feeds of both the feed and permeate sides of the DCMD module for exergy calculations.

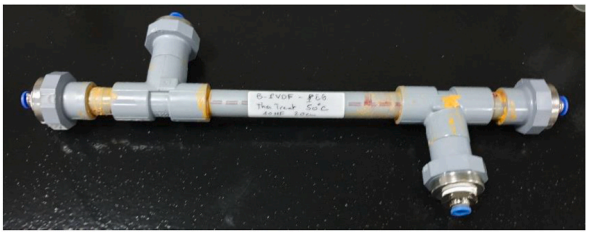

Fig. 1. The cell used in the experiment.

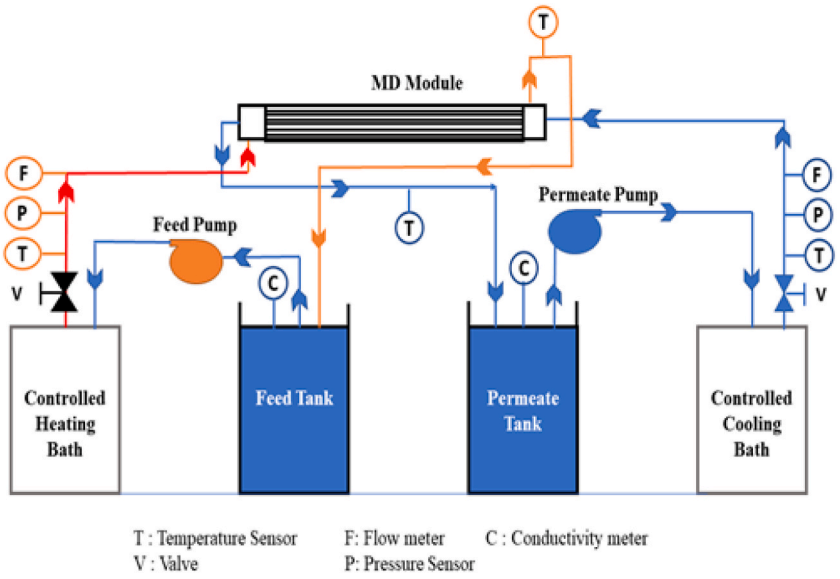

Fig. 2. DCMD performance investigation system for the current study.

Table 2
Physical and chemical characteristics of SWRO brine.

Element	Concentration (ppm)
TDS	45500
Bromide	110.8
Chloride	30971.4
Sulphate	4167.2
Sodium	16814.4
Potassium	532.8
Beryllium	0.001
Selenium	0.38
Magnesium	1770.2
Total Organic Carbons (TOC)	0.26
Calcium	434.8
Zinc	0.280

configuration, the cold permeate is traveling in the hollow fiber membrane and the hot feed is in the cell.

The flux across the membrane can be calculated based on equation (1),

$$\mathcal{J}_v = \frac{\Delta m}{\Delta t \times A} \tag{1}$$

In the above equations, $\mathcal{J}_v$ is the vapor permeate flux, Δm is the mass of permeate, and A is the effective area of the membrane for the time interval Δ*t*.

2.3. Exergy analysis

Using basic exergy definitions and connections for MD models described in the literature, we can find the exergy rates for each stream across the MD system and assess the exergy efficiency of the MD module. Temperatures in the module and the composition of the saline water are the most important characteristics that govern the MD process, whereas potential and kinetic exergies are ignored. As a result, the current streams' exergy rates are equal to the total of chemical and physical exergies given by Equation (2) [14].

$$Ex = Ex_p + Ex_c \tag{2}$$

Where Ex_p refers to the thermochemical exergy based on the temperature of the streams and Ex_c represents the chemical exergy from the solute components in the stream. The physical exergy can be represented in terms of heat entropies and enthalpies at specified conditions (h, s) concerning reference conditions (h_o, s_o) by Equation (3) [14].

$$Ex_p = G[(h - h_o) - T_o(s - s_o)] \tag{3}$$

Where Ex is the exergy [kJ/h], G is the mass flow rate [kg/h], h is the specific enthalpy [kJ/kg], T is the temperature [K] and s is the specific entropy [kJ/K*kg]. The subscript o indicates the reference state that is considered for pure water at T_o and p_o (temperature and pressure of feed water, that is $T_o = 20\ ^\circ C$ $p_o = 0.10$ MPa).

If the intensive parameters that characterize the system are temperature, pressure, and concentration, the exergy can be expressed as follows [12,16]:

$$Ex_p = \frac{p - p_o}{\rho} \tag{4}$$

$$Ex_T = C_p(T - T_o) - C_P T_o \ln\left(\frac{T}{T_o}\right) \tag{5}$$

The equation is used to determine chemical exergy, which is based on chemical potentials or concentrations of the components in the stream (6) [12,16].

$$Ex_C = -N_s \times R \times T_o \times \ln X_s \tag{6}$$

Where:

Cp specific heat of the solution [kJ/kg*K]; Ns moles of solvent per mass unit of the solution $= \frac{\left(1000 - \sum \frac{C_i}{\rho}\right)}{MW_s}$;

X_s mole fraction of the solvent $= \frac{N_s}{\left[N_s + \sum\left(\frac{\beta_i C_i}{\rho MW_i}\right)\right]}$;

β_i number of particles generated from the dissociation of species I; ρ density of the liquid solution [kg/L]; C_i mass concentration of the ith chemical component per liter of solution [g/L]; MW_s, MW_i molecular weight [g/mol] of the solvent s and the chemical component, respectively.

The thermal analysis of DCMD is divided into two parts: feed and permeate. Fig. 3 depicts the temperatures, exergies, mass, and heat inflows and outflows from the feed and permeate sides of both in-out and out-in configurations. The formulae used to calculate the exergy of the streams are listed below [17].

$$Q_1 = 2\pi \times L \times K_1 \times \frac{(T_1 - T_{membtane})}{\ln\left(\frac{r_2}{r_1}\right)} \tag{7}$$

$$Q_1 = 2\pi \times L \times K_2 \times \frac{(T_1 - T_{wall})}{\ln\left(\frac{r_2}{r_1}\right)} \tag{8}$$

Where, in Equations (7) and (8), K_1 and K_2, r_1 and r_2, and L are the thermal conductivities and radius of PVDF membrane and PVC pipe,

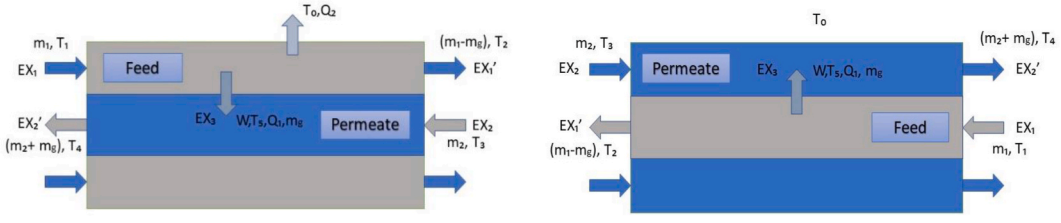

Fig. 3. Exergy analysis for DCMD process.

and the length of the module, respectively as shown in Fig. 4.

$$W_{min} = \sum Ex_{in} - \sum Ex_{out} \tag{9}$$

$$Lost\ work = \sum_{in}\left[EX + Q\left(1 - \frac{T_{surrounding}}{T_{system}}\right) + W\right] - \sum_{out}\left[EX + Q\left(1 - \frac{T_{surrounding}}{T_{system}}\right) + W\right] \tag{10}$$

$$T_5 = \frac{T_3 + T_4}{2} \tag{11}$$

$$W = \int_{V1}^{V2} Pdv \tag{12}$$

$$W = \left(P_{feed} - P_{permeate}\right) \times \left(v_{feed} - v_{permeate}\right) \times \dot{m} \tag{13}$$

$$\dot{m} = A \times J \tag{14}$$

Where P is the pressure in kPa, v is the specific volume in m^3/kg, $\dot{m}$ is the mass flow rate and W is the work of expansion [17].

$$EX_1 = \dot{m}\left(C_p(T_1 - T_o) - C_P T_o \ln\left(\frac{T_1}{T_o}\right) + \frac{(p - p_o)}{\rho} - N_s \times R \times T_o \times \ln(X_{s1})\right) \tag{15}$$

$$EX_1^{'} = \left(\dot{m}_1 - \dot{m}_g\right)\left(C_p(T_2 - T_o) - C_P T_o \ln\left(\frac{T_2}{T_o}\right) + \frac{(p - p_o)}{\rho} - N_s \times R \times T_o \times \ln(X_{s1})\right) \tag{16}$$

$$EX_2 = \dot{m}\left(C_p(T_3 - T_o) - C_P T_o \ln\left(\frac{T_3}{T_o}\right) + \frac{(p - p_o)}{\rho} - N_s \times R \times T_o \times \ln(X_{s2})\right) \tag{17}$$

$$EX_2^{'} = \left(\dot{m}_2 + \dot{m}_g\right)\left(C_p(T_4 - T_o) - C_P T_o \ln\left(\frac{T_4}{T_o}\right) + \frac{(p - p_o)}{\rho} - N_s \times R \times T_o \times \ln(X_{s2})\right) \tag{18}$$

$$EX_3 = \dot{m}_g\left(C_p(T_5 - T_o) - C_P T_o \ln\left(\frac{T_5}{T_o}\right) + \frac{(p - p_o)}{\rho}\right) \tag{19}$$

Where X_{s1} and X_{s2} in the above equations are the mole fraction of solvent at the feed and permeate side of the module, respectively. EX and $EX^{'}$ are the exergies at the input and output of the feed and permeate side of the module, respectively.

2.3.1. Analysis for the feed side of DCMD

The equations for minimum work W_{min} quired in terms of exergy and lost work LW that degrades the energy content of the system at the feed side of the module, are given by,

$$W_{min} = EX_1^{'} - EX_1 + EX_3 \tag{20}$$

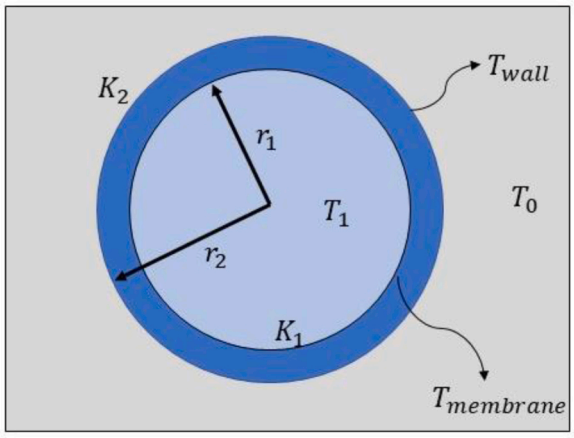

Fig. 4. Heat transfer through pipe and membrane.

$$W = EX_1 - EX_1^{'} - Q_1\left(1 - \frac{T_5}{T_1}\right) - W - Q_2\left(1 - \frac{T_0}{T_1}\right) - EX_3 \tag{21}$$

Exergy efficiency on the feed side of the module is given by

$$\eta_{feed} = \frac{W_{min}}{LW + W_{min}} \tag{22}$$

2.3.2. Exergetic efficiency for permeate side of DCMD

The equations for minimum work W_{min} quired in terms of exergy and lost work LW that degrades the energy content of the system at the permeate side of the module, are given by [17],

$$W_{min} = EX_2^{'} - EX_2 - EX_3 \tag{23}$$

$$W = EX_2 - EX_2^{'} - Q_1\left(1 - \frac{T_1}{T_5}\right) + W + EX_3 \tag{24}$$

And exergy efficiency for permeate stream is as follows,

$$\eta_{permeate} = \frac{W_{min}}{LW + W_{min}} \tag{25}$$

3. Results and discussion

3.1. Permeate flux as function temperature for different module configurations

Fig. 5 and 6 shows the trend of flux versus time, at three different temperatures for out-in and in-out module configuration, respectively. The flux is calculated at three different temperatures for a time interval of 2 h. Increasing the T_f promotes water evaporation, increases the vapor pressure in the feed channel, and eventually increases the permeation flux [19]. The flux across the membrane can find out by using equation (1).

From the flux-temperature graph for the out-in configuration, as in Fig. 5, flux considerably increases with the increase in temperature. For lower temperatures i.e., 44 °C and 55 °C, the flux increases with time and remains almost constant for a specified time. While at a high temperature of 70 °C, flux increase significantly at the start and follows a decrease in flux at the end of a specified time interval due to the increase in concentration. As for flux, its equation is given by

$$\mathcal{J}_v = C\left(P_f - P_P\right) \tag{27}$$

$$P_f = (1 - X_s)P_{sat,w}(x, T) \tag{28}$$

$$P_{sat,w}(x, T) = P_w^o(T)a_w(x) \tag{29}$$

Where P_f and P_p are the pressure at the feed and permeate side, respectively, $P_{sat,w}$ is the partial water vapor pressure in the solution, x is the non-volatile solute mole fraction, T is the absolute temperature and P_w^o is the vapor pressure of pure water determined by Antoine equation [3]:

$$P_{sat,w} = 133.322 \times 10^{\left(8.10765 - \frac{1750.286}{T - 38.15}\right)} \tag{30}$$

As from the above equations, flux changes with the change of vapor pressure and it is in turn the function of temperature. Following

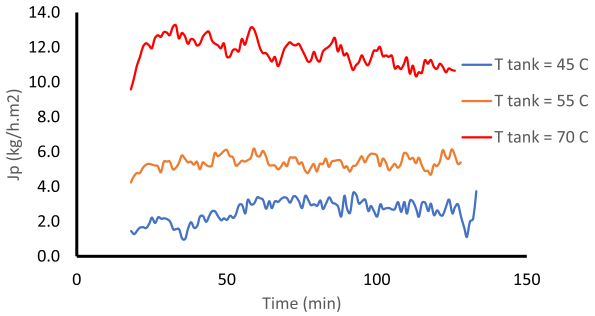

Fig. 5. Relationship between flux rate and change of temperature for out-in module.

the high temperature of 70 °C, the flux increases at first then it shows a decreasing trend. This is because of the increase in salt concentration due to the increase in water recovery rate over time.

For in-out module configuration, the flux-temperature graph, as shown in Fig. 6, shows the same trend of increase of flux with the increase of temperature. But the flux values are lower as compared to that of the out-in module configuration. The highest flux that is obtained in the out-in configuration is 13.3 kg/h.m^2 while it is only 6.23 kg/h.m^2 for the in-out system of the module.

Qu et al., 2015 [20], used the lumen-side and shell-side feed in the membrane distillation process to compare the designs of hollow fiber modules. From experimental work they have done, it is found that the fluxes of different module configurations in shell-side feed operations were found to be lower than in lumen-side feed operations. The module flux rose as the feed flow rate increased, and all of the changed modules showed relatively high flux even at low feed flow rates, indicating that the spacers or wavy geometries improved the fluid flow.

Park et al., 2021 [21], looked at how scale builds up on inside-out and outside-in hollow fiber membrane distillation (MD) modules when hypersaline feed solutions are concentrated. They concluded that under no fouling conditions, the initial flux of the inside-out MD module was marginally higher than that of the outside-in MD module. However, under identical operating conditions, the inside-out MD modules had a faster reduction in flux due to scale formation than the outside-in MD modules.

3.2. Feed concentrations as function temperature for different module configurations

Fig. 7 and Fig. 8 indicates the effect of the change of feed concentration with temperature change for the specific time interval for out-in and in-out module configuration, respectively. In this figure total dissolved solids (TDS) are plotted with changing temperature for a specified interval of time.

There is an increase in feed concentration for each temperature given for both out-in and in-out module configurations. And the TDS shows greater values against temperatures for the out-in system of the module as compared to in-out. It is because the axial speed is higher in out-in configuration as compared to in-out i.e., 155.16 kg/h and 47.53 kg/h respectively. So as the axial speed increases with temperature, does the flux and the TDS at the feed side [22]. The out-in system of the module, with the high temperature of 70 °C has a TDS increment faster than the other two given temperatures, which jumps from almost 47 g/l to 51 g/l within a time interval of 2 h. While for the other two temperatures i.e., 44 °C and 55 °C TDS remains in between 47 and 48 g/l. From the graph of TDS for the out-in module system as in Fig. 7, as the temperature of the feed side increases, it results in increases in the recovery rate of water, as a result, salt concentration also increases. It shows highest at 70 °C. The same kind of trend can be seen for in-out module configuration as shown in Fig. 8.

3.3. Exergy change as function temperature for different module configurations

Using the equations of exergy analysis, as discussed in the methodology section, exergies for both in-out and out-in configurations at the in-feeds and out-flows of both the feed and permeate side of the DCMD module have been calculated. These calculations considered both physical and chemical exergies as changes with temperature. Fig. 9 and 10 shows the total change of exergy in the module for out-in and in-out module configurations, respectively.

Exergy change in any system is the difference between the total amount of heat content that is entering the system to that of heat content leaving that system. As in our system, we are considering only the membrane module for the study of exergy change, so the feed enters the system at high temperatures and after an exchange of heat with the membrane and with the outside of the module, it leaves at a lower temperature. On the other hand, the permeate, which is the cold side of the membrane, enters the system at a lower temperature and leaves at high temperatures. And their difference, the exergy of streams entering the module to that of leaving the module, is the total exergy change in the module.

So, from Fig. 9, for out-in module configuration, at high feed temperatures, the change of exergy is higher as compared to lower feed temperatures. And this exergy changes at 70 °C, is almost 6 folds as compared to exergy changes at 55 °C which is only 3 folds with

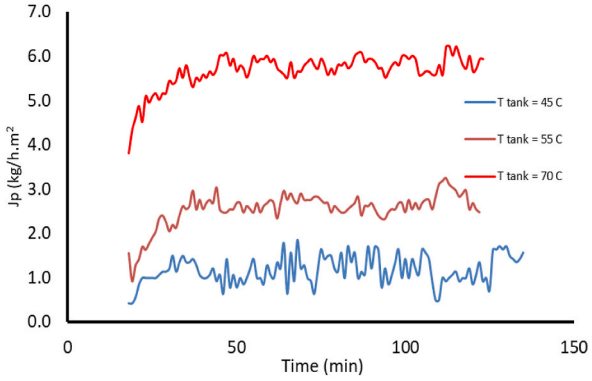

Fig. 6. Relationship between flux rate and change of temperature for in-out module.

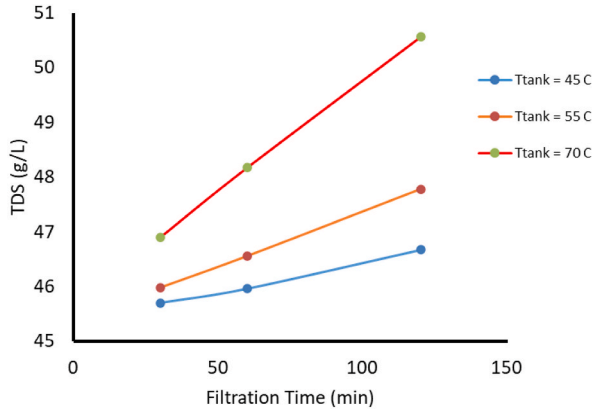

Fig. 7. Effect of change of temperature on TDS of feed for out-in module.

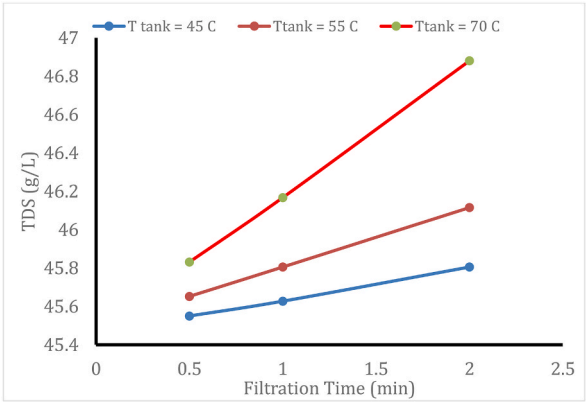

Fig. 8. Effect of change of temperature on TDS of feed for in-out module.

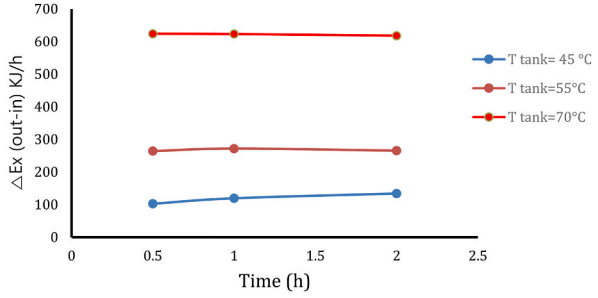

Fig. 9. Exergy change for out-in module configuration.

that of at 45 °C, which is only 100 kJ/h. The highest exergy change for the system is at 70 °C, which is 624 kJ/h.

As compared to the out-in configuration, the in-out system has lower amount of exergy, this is because the hot feed now travels in the hollow fibers membranes, as shown in Fig. 10, so it has less mass flow area as compared to the out-in system. Also, in the in-out system, it isn't in contact with the outside system, so no heat is lost in that case also. While in the out-in configuration, the hot feed also lost its heat to the outside medium of the system due to thermal conduction, which cause an increase in the exergy change of the system.

The same trend can be seen for the in-out system, as high feed temperatures cause high exergy to change. On the other hand, exergy changes less at lower feed temperatures.

It is worth mentioning here that about 50 %–80 % of energy is consumed as latent heat for producing water vapor, while the remaining is lost by thermal conduction.

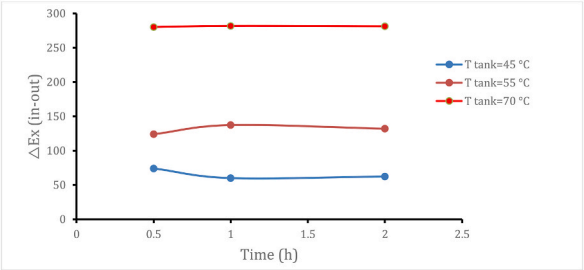

Fig. 10. Exergy change for in-out module configuration.

3.4. *Exergetic efficiency of feed as function temperature for different module configurations*

Fig. 11 shows the exergetic efficiency for the out-in feed flow concerning temperature change. As there is an increase of efficiencies for the given increase of feed temperatures with changing time intervals, for high feed temperature of 70 °C, has the highest efficiency of 71.94, as compared to low temperatures of 45 °C and 55 °C. This is because the water permeability of a porous membrane used in DCMD is governed by the Knudsen-Molecular diffusion mechanism when the mean pore size lies between 0.2 and 1 μm [3].

The quantity which governs the operative mechanism for a given membrane pore under specific experimental conditions is the Knudsen number (*Kn*), which is defined as:

$$Kn = \frac{\lambda_w}{d_p} \tag{31}$$

Where d_p is the membrane pore size and λ_w is the mean free path of water molecules in the vapor phase, is given by the following expression,

$$\lambda_w = \frac{k_B T}{\sqrt{2} P_m \left(2.641 \times 10^{-10}\right)^2} \tag{32}$$

Where k_B is the Boltzmann constant, P_m is the mean pressure within membrane pores and T is the absolute temperature.

Knudsen type flow is responsible for the mass transfer through the membrane pores, which is increased with the increase of temperature, as the collisions of water vapors with that of membrane surface increase with the increase of temperature, which increases feed efficiency of the module.

Fig. 12 shows the feed efficiencies of the in-out configuration at different temperatures at different time intervals. It shows the trend of increase in feed efficiency with an increase in temperature, as in the out-in system. But their efficiency values are lower as compared to that of the out-in configuration. As of now in this case, the hot feed is inside the hollow fiber membranes, and permeate travels outside it, so hot feed has a lower mass flow rate (around 48 kg/h) as compared to the permeate flow rate (around 147 kg/h). This results in lower heat transfer rates and flux rates.

3.5. *Exergetic efficiency of permeate as function temperature for different module configurations*

Fig. 13 depicts the exergetic efficiency of the permeate side for out-in configuration with changing temperature as a function of time. From the graph, permeate efficiency is higher at lower feed temperatures as compared to higher temperatures. At higher temperatures, the feed tends to transport more distilled water as compared to lower temperatures. This is because as the water vapors travel from the feed side to the permeate side of the membrane through membrane pores, the concentration of non-volatile solutes at the membrane surface becomes higher than the concentration in the bulk feed aqueous solution, which leads to concentration polarization phenomenon and results into reduction in both the driving force and the permeate DCMD flux [3]. And so does the permeate efficiency. The permeate efficiency is highest at 45 °C is 31.42 %.

Fig. 14 indicates the permeate efficiencies for the in-out configuration of the module at different feed temperatures at different time intervals. It can observe from the graph that at lower feed temperatures, the in-out module configuration shows higher efficiency rates as compared to the out-in configuration. This is because, at low feed temperatures, the concentration polarization phenomenon is less likely to be significant as compared to high feed temperatures. Also, in the in-out configuration, the hot feed is confined inside hollow fiber membranes, and feed mass flow rates have lower values as compared to permeate mass flow rates, which results in fewer effects on permeate temperatures.

4. Conclusion

DCMD has an excellent ability to lower the volume of desalination brine coming from the RO plant while producing more freshwater. In this study, the exergy analysis of a laboratory scale direct contact membrane distillation unit with different module configurations, i.e. inlet-outlet and outlet-inlet, processing desalination brines, is done, as well as the effect of supply temperatures on

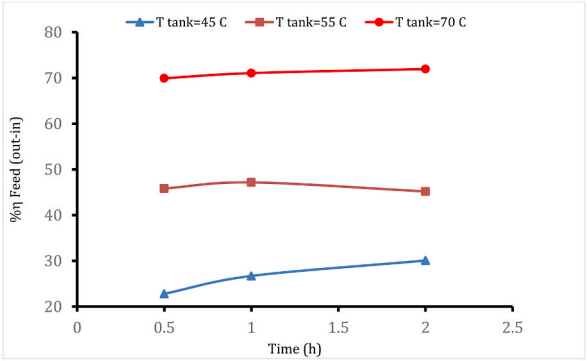

Fig. 11. Exergetic Efficiency of feed for out-in module configuration.

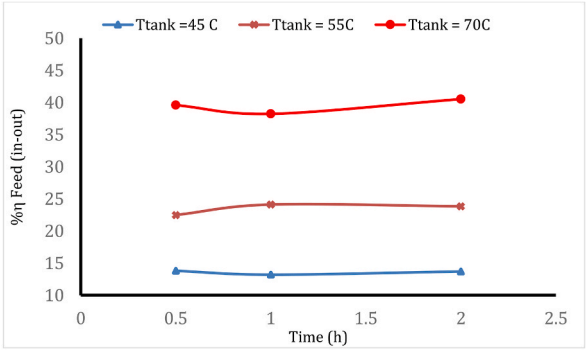

Fig. 12. Exergetic Efficiency of feed for in-out module configuration.

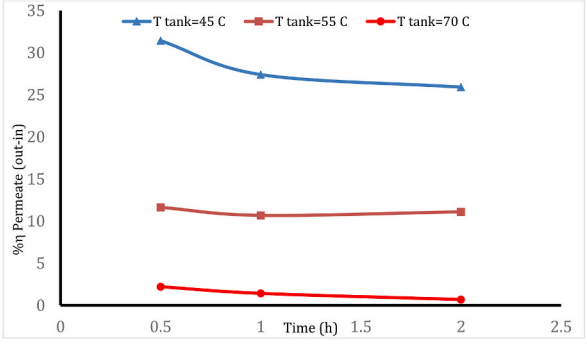

Fig. 13. Exergetic Efficiency of permeate for out-in module configuration.

flux with a variable time interval. The results showed that with the increase in feed temperature, there is an increase in water flow through the membrane for both kinds of module configurations. However, the rate of flux for an outside-in system of the module has greater values as compared to an inside-out. The same type of increasing trend can be seen for TDS at the feed side of the membrane. This is because at higher temperatures, the rate of evaporation increases at the feed side of the membrane which increases flux rates. The maximum fluxes obtained at 70 °C are 13.3 kg/h.m^2 for the out-in configuration and 6.23 kg/h.m^2 for the in-out.

The total exergy changes inside the membrane module at both the feed and permeate sides of the membrane, as well as the exergetic efficiency of the feed and permeate sides, are included in the exergy analysis. Exergy changes for both membrane modules increase with the increase in temperature. It is because the greater the temperature, the greater the heat transfer/loss through the membrane to the permeate side of the membrane, increasing permeate temperature and also heat lost outside of the membrane with the outside medium. The exergy changes and exergetic efficiency of the hot feed, for the out-in module configuration, are greater than the in-out module configuration. This is because in out-in module configuration the hot feed is in the shell side of the module and has greater flow rates as compared to in-out. So, it shows greater heat transfer rates and as a result change of exergy increases.

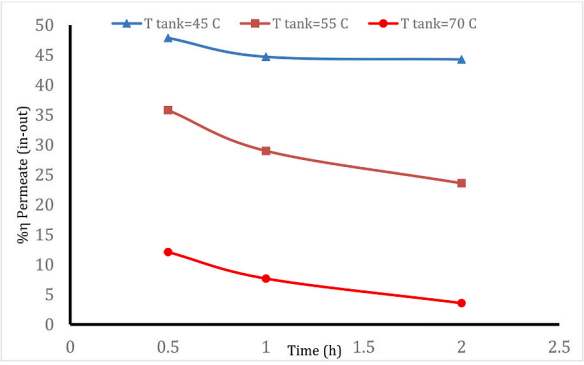

Fig. 14. Exergetic Efficiency of permeate for in-out module configuration.

The exergetic efficiency of cold permeate has a greater percentage at lower temperatures than at higher temperatures for both out-in and in-out module configurations. This is because as the vaporization at the feed side of the module increases, so does the salt concentration on the feed side closer to the membrane surface, which leads to the concentration polarization effect. So greater the temperatures, results to higher concentration polarization. Which in return, lowers the exergetic efficiency of the permeates.

However, several limitations should be acknowledged also in this study while discussing exergy in DCMD. DCMD systems have many variables, heat and mass transport mechanisms, and non-linear behavior. Exergy study uses simplified models and assumptions that may not accurately represent DCMD. DCMD complexity can reduce exergy analysis accuracy and dependability. Furthermore, the lack of a standardized methodology impedes comparability between different studies. Despite these aforementioned limitations, exergy analysis retains its value in optimizing DCMD processes and comprehending their thermodynamic characteristics.

Declaration of competing interest

The authors declare that they have no known competing financial interests or personal relationships that could have appeared to influence the work reported in this paper.

Acknowledgments

The authors extend their appreciation to the Deputyship for Research and Innovation, Ministry of Education in Saudi Arabia, for funding this research work through the project number (632).

References

[1] The urgency for water desalination. https://www.acwapower.com/news/the-urgency-for-water-desalination/. (Accessed 6 January 2022).
[2] C. Huayan, W. Chunrui, J. Yue, W. Xuan, L. Xiaolong, Comparison of three membrane distillation configurations and seawater desalination by vacuum membrane distillation, Desalin. Water Treat. 28 (1–3) (2011) 321–327, https://doi.org/10.5004/dwt.2011.1605.
[3] M. Khayet, T. Matsuura, "Chapter 10 – direct contact membrane distillation", membrane distillation, Principles and Applications (2011) 249–293, https://doi.org/10.1016/B978-0-444-53126-1.10010-7.
[4] Y. Zhang, J. Sun, F. Guo, Performance enhancement for membrane distillation by introducing insoluble particle fillers in the feed, Desalination 558 (2023), 116624, https://doi.org/10.1016/j.desal.2023.116624.
[5] B.L. Pangarkar, M.G. Sane, M. Guddad, Reverse osmosis and membrane distillation for desalination of groundwater: a review, ISRN Mater. Sci. 2011 (2011) 1–9, https://doi.org/10.5402/2011/523124.
[6] I.D. Luna-Santander, R.M. Gómez-Espinosa, A. García-Bórquez, B. Torrestiana-Sánchez, Enhancement of heat and mass transfer in the DCMD process using UV-assisted 1-hexene-grafted PP membranes, ACS Omega 7 (49) (2022) 44903–44911, https://doi.org/10.1021/acsomega.2c05075.
[7] Z. Anari, A. Sengupta, K. Sardari, S.R. Wickramasinghe, Surface modification of PVDF membranes for treating produced waters by direct contact membrane distillation, Sep. Purif. Technol. 224 (2019) 388–396, https://doi.org/10.1016/j.seppur.2019.05.032.
[8] F. Banat, N. Jwaied, Exergy analysis of desalination by solar-powered membrane distillation units, Desalination 230 (1–3) (2008) 27–40, https://doi.org/10.1016/j.desal.2007.11.013.
[9] E. Jansen, A. E, J.W. Assink, J.H. Hanemaaijer, J. van Medevoort, van Sonsbeek, Development and pilot testing of full-scale membrane distillation modules for deployment of waste heat, Desalination 323 (2013) 55–65, https://doi.org/10.1016/j.desal.2012.11.030.
[10] D. Woldemariam, A. Kullab, U. Fortkamp, J. Magner, H. Royen, A. Martin, Membrane distillation pilot plant trials with pharmaceutical residues and energy demand analysis, Chem. Eng. J. 306 (15) (2016) 471–483, https://doi.org/10.1016/j.cej.2016.07.082.
[11] D. Woldemariam, A. Martin, M. Santarelli, Exergy analysis of air-gap membrane distillation systems for water purification applications, Appl. Sci. 7 (3) (2017) 301, https://doi.org/10.3390/APP7030301.
[12] F. Macedonio, E. Drioli, L. Gzara, Water and salts recovery from desalination brines an exergy evaluation, J. Env. Chem. Eng. 9 (5) (2021), 105884, https://doi.org/10.1016/j.jece.2021.105884.
[13] M.S. Sri Abirami Saraswathi, D. Rana, N.J. Kaleekkal, K. Divya, A. Nagendran, Investigating the efficacy of PVDF membranes customized with sulfonated graphene oxide nanosheets for enhanced permeability and antifouling, J. Environ. Chem. Eng. 8 (5) (2020), 104426, https://doi.org/10.1016/j.jece.2020.104426.
[14] R. Molinari, R. Gagliardi, E. Drioli, Methodology for estimating saving of primary energy with membrane operations in industrial processes, Desalination 100 (1–3) (1995) 125–137, https://doi.org/10.1016/0011-9164(96)00014-8.
[15] Y. Cerci, Exergy analysis of a reverse osmosis desalination plant in California, Desalination 142 (1–3) (2002) 257–266, https://doi.org/10.1016/S0011-9164(02)00207-2.

[16] F. Macedonio, E. Drioli, An exergetic analysis of a membrane desalination system, Desalination 261 (3) (2010) 293–299, https://doi.org/10.1016/j.desal.2010.06.070.
[17] M.M.A. Fakron, Energy and exergy analysis and modeling temperature distribution in a membrane distillation feed channel for VMD and DCM, IDA J. Desalin. Water Reuse 6 (3–4) (2014) 121–127, https://doi.org/10.1179/2051645214Y.0000000031.
[18] C. Jihyeok, C. Yongjun, Y. Kim, L. Sangho, Exergy analysis of a direct contact membrane distillation (DCMD) system based on computational fluid Dynamics (CFD), Membranes 11 (7) (2021) 525, https://doi.org/10.3390/membranes11070525.
[19] D.U. Lawal, A.E. Khalifa, Flux prediction in direct contact membrane distillation, Int. J. Mater. Mech. Manuf. 2 (4) (2014) 302–308, https://doi.org/10.7763/ijmmm.2014.v2.147.
[20] D. Qu, T. Zhou, W. Ma, Z. Peng, Z. Li, M. Qin, Comparison of hollow fiber module designs in membrane distillation process employed lumen-side and shell-side feed, Desal. Wat. Treat. 57 (17) (2016) 7700–7710, https://doi.org/10.1080/19443994.2015.1049561.
[21] Y. Park, Y. Choi, J. Choi, J. Ju, D. Kim, S. Lee, Comparison of scale formation between inside-out and outside-in hollow fiber membrane distillation (MD) modules when concentrating hyper saline feed solutions, Desal. Wat. Treat. 157 (2019) 372–382, https://doi.org/10.5004/dwt.2019.24357.
[22] M. Khayet, C. Cojocaru, C. García-Payo, Application of response surface methodology and experimental design in direct contact membrane distillation, Ind. Eng. Chem. Res. 46 (17) (2007) 5673–5685, https://doi.org/10.1021/ie070446p.